

Chemical Composition and Genesis of Ferromanganese Crusts from the Sonne Ridge (Kuril Basin, Sea of Okhotsk)

Yu.M. Ivanova^{a, ✉}, P.E. Mikhailik^{a,b}, E.V. Mikhailik^a, N.V. Zarubina^a, M.G. Blokhin^a

^a Far Eastern Geological Institute, Far Eastern Branch of the Russian Academy of Sciences,
pr. 100-letiya Vladivostoka 159, Vladivostok, 690022, Russia

^b Far Eastern Federal University, ul. Sukhanova, 8, Vladivostok, 690950, Russia

Received 2 March 2018; received in revised form 3 September 2018; accepted 8 November 2018

Abstract—The paper presents results of a comprehensive study of ferromanganese crusts from a submarine volcano on the Sonne Ridge, which was discovered during the 178th cruise of the RV Sonne (2004) investigating the northern slope of the Kuril basin in the framework of the KOMEX program. Results of study of the structures, textures, and mineral and elemental compositions of the crusts suggest their hydrogenous origin. The contents of major, trace, and rare-earth elements and Y (REY) in four mineral phases of ferromanganese crusts of the Sea of Okhotsk have been determined by phase analysis for the first time. The REY patterns of the manganese and ferrous in-situ phases confirms the hydrogenous genesis and indicates no hydrothermal influence.

Keywords: selective leaching, ferromanganese crusts, Sonne Ridge, submarine volcano, Sea of Okhotsk

INTRODUCTION

Ferromanganese deposits (FMD) are rather common at the world's ocean floor, where they form gigantic deposits of crusts and nodules (Baturin, 1993; Andreev, 1994; Anikeeva et al., 2002; Andreev et al., 2007).

At present, much less data is available on composition and genesis of FMD in marginal seas than in the open part of the Ocean. Thus, the research in these areas appears to be topical and sought for in terms of developing a general theory of oceanic ferromanganese ore genesis, which would include identifying the peculiarities of metallogenic zoning of the ocean floor in the NW Pacific.

The first studies of FMD in far eastern marginal seas of Russia showed that they were vastly represented by hydrothermal differences, while the hydrogenous and diagenetic ones constituted a much smaller part (Shterenberg et al., 1986). However, the studies of FMD in the Sea of Okhotsk and the Sea of Japan showed that, in addition to hydrothermal ferromanganese crusts, hydrogenous and diagenetic FMD were encountered rather often (Mikhailik et al., 2016).

FMD formation under conditions of near-continental lithogenesis is distinguished by increased terrigenous components, which makes it more difficult to draw conclusions on genesis of FMD after bulk composition investigations. The information on the origin of marine minerals is carried by their authigenic mineral phases. It is known that FMD com-

prise four mineral phases represented by intergrown manganese oxides (MnO_2) and iron hydroxides ($FeOOH$), as well as carbonate and residual aluminosilicate phases. Mineral phases are studied using method of sequential leaching. This technique proved effective in studying hydrothermal ferromanganese crusts from a submarine volcano in the Sea of Japan. The investigation resulted in a more detailed understanding of the genesis of mineral phases, based on which ore crusts could be attributed to the hydrothermal-sedimentary type (Mikhailik et al., 2017). The next step of our comprehensive research focused on the target in the Sea of Okhotsk, where FMD have been known since late last century. Their samples were recovered during the 21st and the 27th cruises of the RV Pegas in 1980 and 1984, respectively, during the 11th, 15th, 17th, and 40th cruises of the RV Vulkanolog between 1981 and 1991, during the 28th cruise of the RV Akademik Lavrentiev in 1998, etc. Most of FMD samples were dredged from the slopes of submarine volcanoes of the Kuril Island Arc, and the rest from seamounts and uplifts in the central part of the Sea of Okhotsk (Kashevarov Bank, Kashevarov Trough, the Academy of Sciences Rise, the Institute of Oceanology Rise, etc.) (Gavrilenko and Khramov, 1986; Uspenskaya et al., 1989; Gavrilenko, 1997; Astakhova and Sattarova, 2005; Glasby et al., 2006; Astakhova, 2007; Anikeeva et al., 2008; Mikhailik et al., 2009; Baturin et al., 2012).

The FMD from submarine volcanoes of the Kuril Island Arc are the ones most researched. Ferromanganese crusts are rather common in this seafloor area, volcanogenic clastic rocks cemented by Mn oxides are less common, and dough-

✉ Corresponding author.

E-mail address: miralda70@mail.ru (Yu.M. Ivanova)

nut-shaped concretions are even rarer (Uspenskaya et al., 1989). The results of investigating into FMD morphology and their mineral and chemical compositions showed that they were primarily of hydrothermal nature, whereas the nodules had diagenetic origin (Gavrilenko, 1997; Uspenskaya et al., 1989; Anikeeva et al., 2008).

The FMD from the central part of the Sea of Okhotsk, where thin ferromanganese crusts are dredged from the slopes of submarine volcanoes of the Kashevarov Bank and the Academy of Sciences Rise and are also encountered in the form of films on barite hills of the Derugin basin and thin crusts at a distance from them, are less well studied (Astakhova, 2007, 2009). The analysis of the data available allowed N.V. Astakhova to accept the hydrothermal nature of their formation. At the same time, thick ferromanganese crusts were recovered from a seamount of tectonic origin in the Kashevarov Trough (Dullo et al., 2004), which revealed their hydrogenous genesis upon analysis (Mikhailik et al., 2009).

In 2004, joint research was carried out in the Sea of Okhotsk by RV Sonne (178th cruise) under the Russian-German project KOMEX (Dullo et al., 2004), which resulted in

the discovery of the previously unknown volcanic chain in the Kuril basin (Fig. 1) later named Sonne Ridge. Ferromanganese crusts were recovered from one of its volcanoes. The goal of the present paper is to demonstrate the results of both bulk compositions samples and mineral phases of ferromanganese crusts from the Sonne Ridge to understand their genesis.

MATERIALS AND METHODS

The material for research was a ferromanganese crust up to 4 cm thick dredged (station SO178-5-4 with dredging interval 47°54.02–47°54.32 N 147°49.11–147°49.29 E; at depth interval 2346–2201 m) from the northern slope of the Kuril basin, Volcano 1 (Fig. 1, test site I). Two samples were selected for the study: SO178-5-4/1 from the lower part of the Fe–Mn crust and SO178-5-4/2 from the upper part.

Volcano 1 (Fig. 2) is located at the depth of ~ 2500 m and rises by about 250 m above the surface. This structure is shaped as an oval elongated in the NS direction with sizes

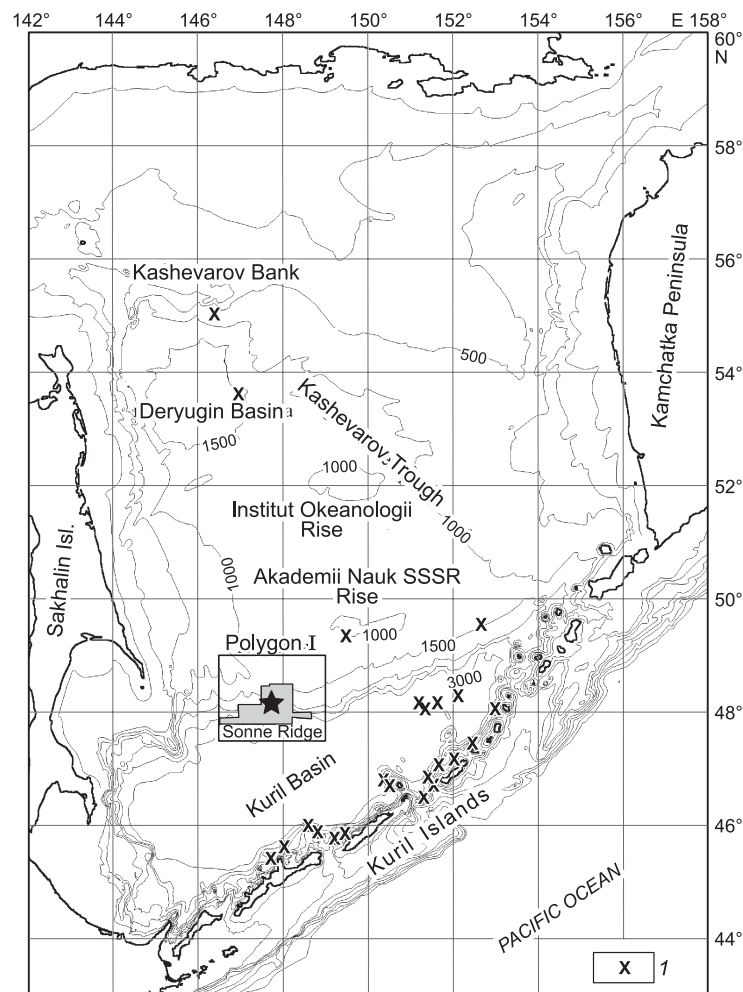


Fig. 1. Location of Area I on the northern slope of the Kuril basin in the Sea of Okhotsk. I, location of ferromanganese deposits (Astakhova and Sattarova, 2005; Astakhova, 2007).

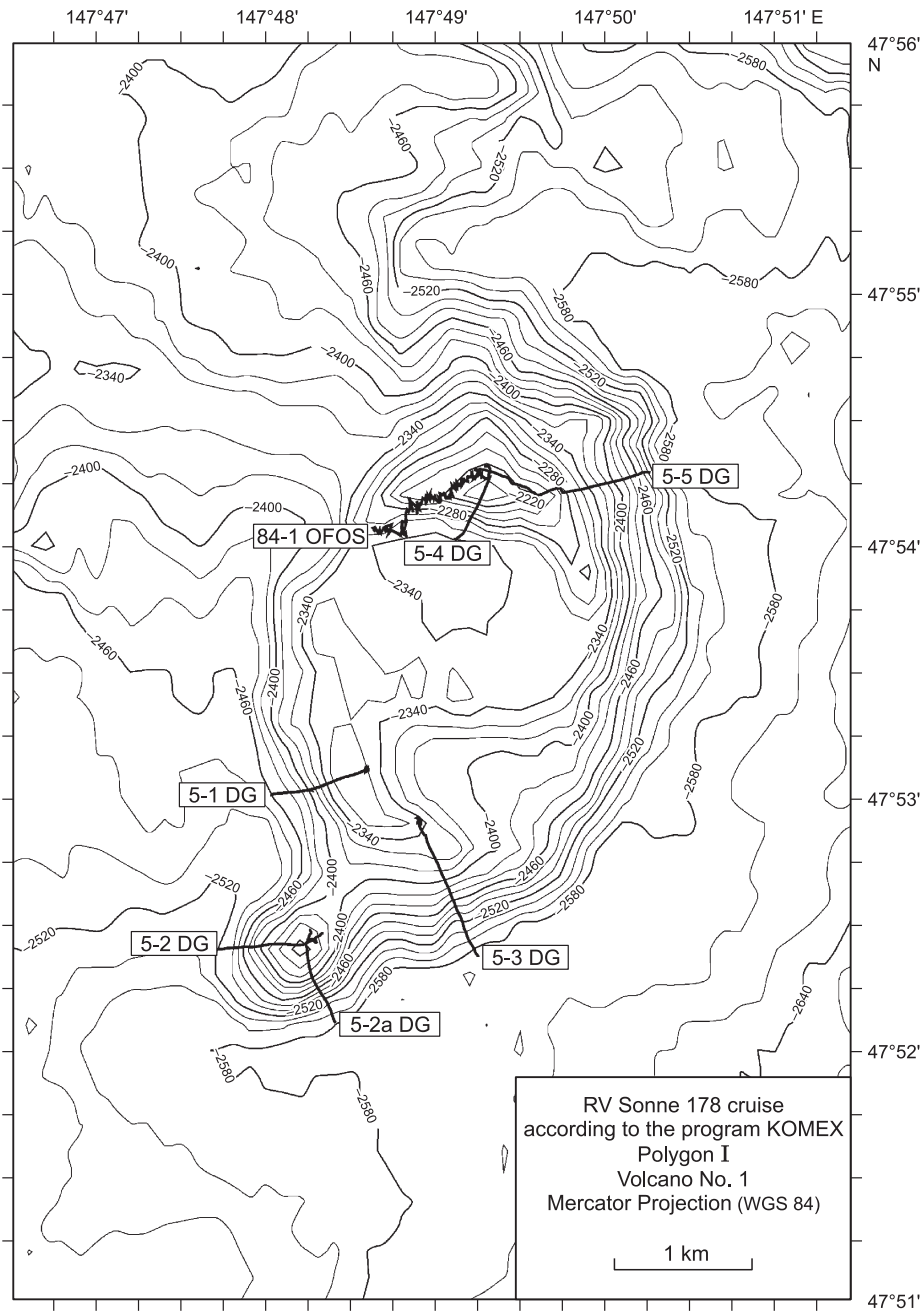


Fig. 2. Bathymetric map of Volcano 1. DG, dredging stations, OFOS, telephoto profiling line. Isobath is 20 m.

~4.5 × 2.5 km at its base. A small cone-shaped hill in the southwest is most likely a satellite. The central part of the volcano is similar to a plateau. A sharp-pointed cone with a steep southern slope is located in the northern part of the structure. Thus, the volcanic structure may be represented by the old volcanic cone destroyed as a result of explosive volcanic activity or tectonic processes (Dullo et al., 2004).

The mineral composition was studied by X-ray powder diffractometry using the MiniFlex II (Rigaku Corporation, Japan). X-ray diffraction analysis was performed using Cu-K α radiation. The X-ray tube voltage was 30 kV, and the

current was 15 mA. The continuous scan rate was 1° 2 θ /min. The 2 θ scan range was 2.5° to 60°. The device was also equipped with Ni selective absorption filter for suppressing K β lines. The qualitative phase composition was assessed using the ICDD 2010 database.

The chemical composition was studied using a number of methods as follows: ICP-AES was used to determine Ti, Al, Fe, Mn, Mg, Ca, Na, K, and P contents; ICP-MS was used to determine Li, Be, Sc, V, Cr, Co, Ni, Cu, Zn, Ga, As, Rb, Sr, Y, Zr, Nb, Mo, Cd, Cs, Ba, REE, Hf, Ta, W, Tl, Pb, Th, and U contents; Si content was identified via gravimetry.

ICP-AES measurements were performed using an iCAP6500 Duo spectrometer (Thermo Scientific, USA). The device was calibrated using the multielement standard solution ICP Multi Element Standard IV (Merck, Germany), ICP-MS was carried out using the Agilent 7700x quadrupole mass spectrometer (Agilent Technologies, Japan). The sample analysis results were assessed and quality controlled based on standard samples of ferromanganese concretion compositions: OOPE 601 (GSO5373-90) and OOPE 602 (GSO 5374-90).

Decomposition of the studied FMD samples to identify bulk contents of elements was performed via open acid digestion by the mixture of supra pure acids HF : HNO₃ : HClO₄.

Distribution of chemical elements by mineral phases was studied based on the data obtained using the sequential leaching technique described in detail in (Mikhailik et al., 2017).

With the phase analysis completed, the results obtained for the bulk sample were compared to the sums of four FMD phases. The mismatch did not exceed 10%, which implies the validity of the analytical approaches applied (Zarubina et al., 2014).

The correctness of the technique was verified by performing X-ray structural analysis of the sample each time after the substance was treated with the reactive agent. Diffraction patterns for initial samples SO178-5-4/1 and SO178-5-4/2 are presented in Fig. 3. It can be seen in the latter example, that treatment with the first reactive agent (1N acetate buffer, pH = 5) does not lead to destruction of the main minerals (Fig. 4a). Although destruction of manganese minerals can be observed after the second treatment of the sample with 0.5M hydroxylamine hydrochloride (pH = 2) (Fig. 4b), and the presence of amorphous phase represented by iron hydroxides can be seen. When the sample is treated with 0.2M oxalate buffer (pH = 3.5), which leads to extraction of authigenic iron and its associated elements, the amorphous phase disappears (Fig. 4c), and only allothigenic aluminosilicates remain.

All analytical studies in the present paper were carried out in the Common Use Center of the Far Eastern Geologi-

cal Institute of the Far Eastern Branch of the Russian Academy of Sciences.

RESULTS

Ferromanganese crusts from the Sonne Ridge are represented by light-brown samples, and the crust substrate by light gray volcanoclastic rocks with ginger-brown deposit and impregnations of dark-colored minerals. One substrate-free sample with a wavy knobby surface (Fig. 5a) was chosen for investigation. The lower part of crusts is darker (Fig. 5b), which indicates the lower quantity of the allothigenic impurity.

Ferromanganese crusts have thin-layer textures with lenticular zones due to the presence of clay impurities. They also have a globular structure and fine-reticulate, fibrous ultrastructure. Some samples display an organogenic structure due to the presence of diatom valves. Fragments of non-metallic minerals with various degrees of roundness were observed. This internal structure is typical for hydrothermal ferromanganese crusts of seamounts and elevations of the World Ocean (Anikeeva et al., 2002).

The X-ray diffraction results show that ferromanganese crust samples from the Sonne Ridge are formed by vernadite (Fig. 3a, b). Moreover, the sample recovered from the surface is different from the one from the base, as it includes a larger amount of terrigenous material represented by quartz and plagioclase, which can be clearly seen in diffraction patterns.

Contents of major elements (Mn, Fe, etc.), microelements (Co, Ni, Zn, Cu), rare earth elements and Y (REY), and other trace elements in bulk samples, as well as Mn/Fe, (Mn + Fe)/Ti, and Y/Ho ratios, and, Y, Ce, and Eu anomalies in ferromanganese crusts of the Sonne Ridge are presented in Table 1. The data on compositions of hydrothermal crusts from the Sea of Japan and FMD from underwater seamounts of the World Ocean are presented in the table as well.

Mn content varies from 17.9 to 29.6%, and Fe content from 13.6 to 16.1%, which on average amount to 23.8 and

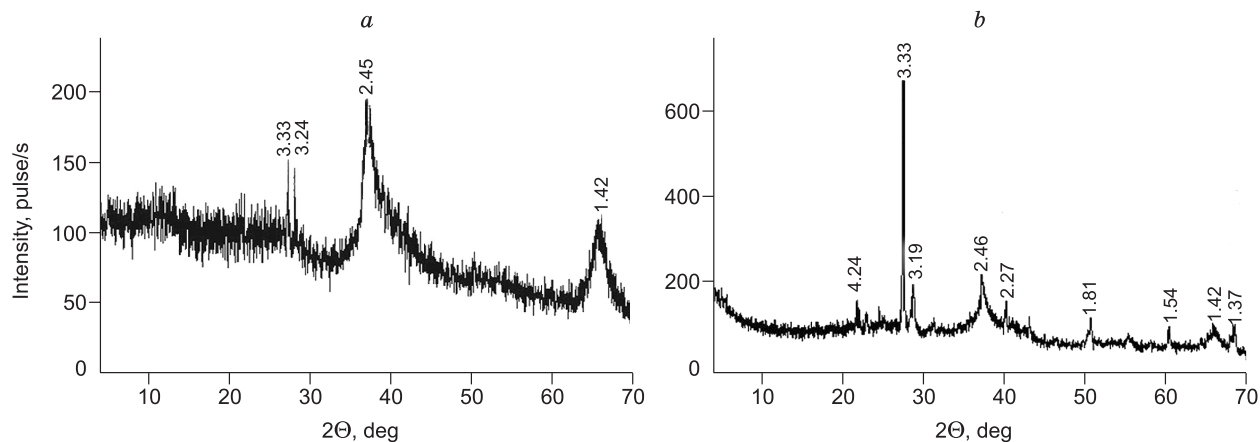


Fig. 3. X-ray diffraction pattern of the sample, bulk composition. *a*, SO178-5-4/1; *b*, SO178-5-4/2. Vernadite, Å, 1.42, 2.45, 2.46; quartz, Å, 1.37, 1.54, 1.81, 2.27, 3.33, 4.24; plagioclase, Å, 3.19, 3.24.

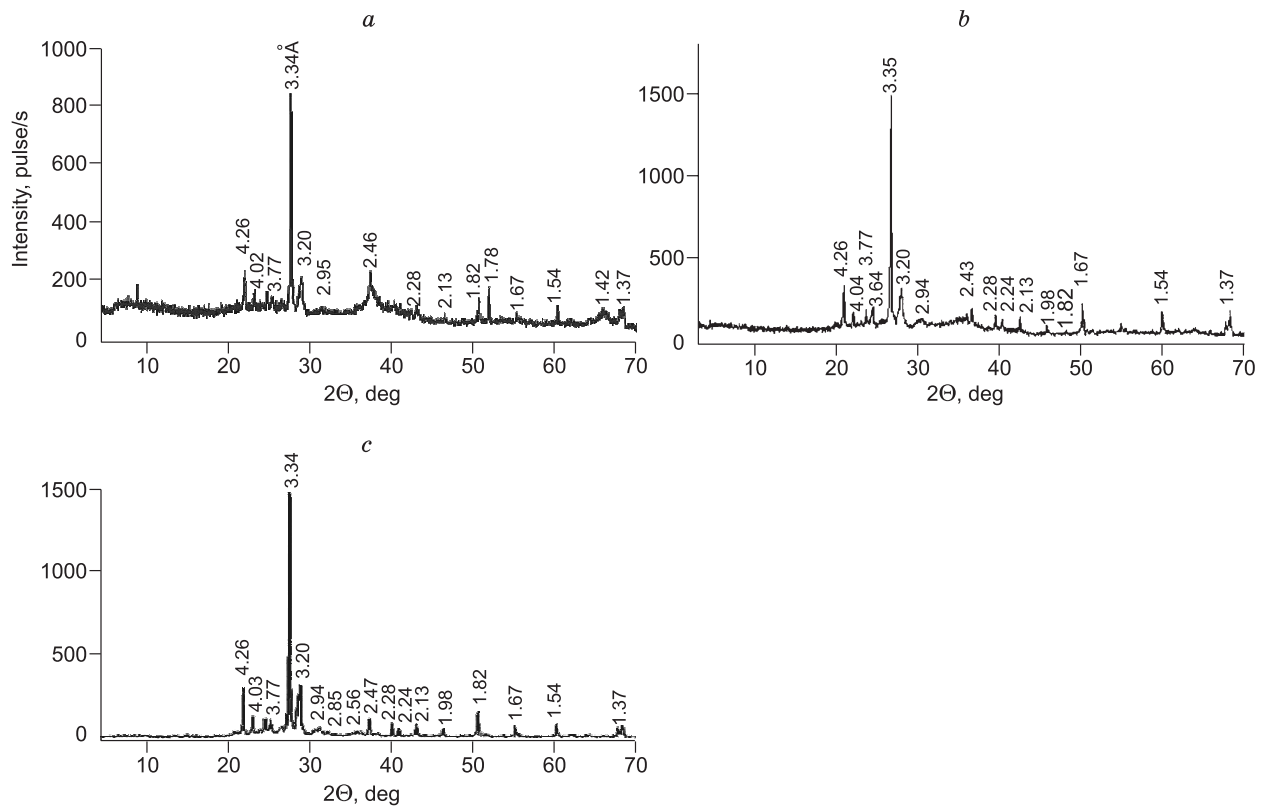


Fig. 4. X-ray diffraction pattern of sample SO178-5-4/2. *a*, After the extraction using acetate buffer; *b*, after the extraction using 0.2 M solution of hydroxylamine hydrochloride; *c*, after the extraction using oxalate buffer. Vernadite, Å, 1.42, 2.46; quartz, Å, 1.37, 1.54, 1.67, 1.82, 1.98, 2.13, 2.24, 2.28, 2.43, 2.47, 2.56, 3.34, 3.35, 4.26; plagioclase, Å, 1.78, 2.85, 2.94, 2.95, 3.20, 3.64, 3.77, 4.02, 4.03, 4.04.

14.9%, respectively. These ranges of Mn and Fe contents are also typical for average values in hydrogenous ferromanganese crusts of the Pacific Ocean (Anikeeva et al., 2002). The studied FMD of the Sonne Ridge show relatively low Si contents (from 4.05 to 11.1). Mn/Fe relation vary from 1.11 to 2.18, which is typical for hydrogenous marine deposits, while the values (Mn + Fe)/Ti (68.6 and 110) indicate the influence of the hydrothermal component and thus do not provide an unambiguous answer regarding the nature of the crusts.

The Co content in ferromanganese crusts of the Sonne Ridge (1801 and 684 ppm) is lower, than in hydrogenous crusts of the Pacific Ocean (2800–12,000 ppm), while Ni

content (3273 and 9120 ppm) is higher, as the oceanic Ni contents are 2200–6300 ppm (Baturin, 1993). It is worth noting that increased Ni contents in the crusts of the Sea of Okhotsk were observed earlier as well (Astakhova, 2007). Although these Ni contents are significantly lower than those in Ni-rich concretionary ores of the Clarion–Cliperton zone (13,900–19,300 ppm), and lean ores of the Central Pacific (7600–12,000 ppm) (Anikeeva et al., 2002). Cu contents (416 and 616 ppm) are lower than in ferromanganese crusts of seamounts and uplifts, as well as nodule fields, but higher, than the average values for hydrothermal deposits (Table 1).

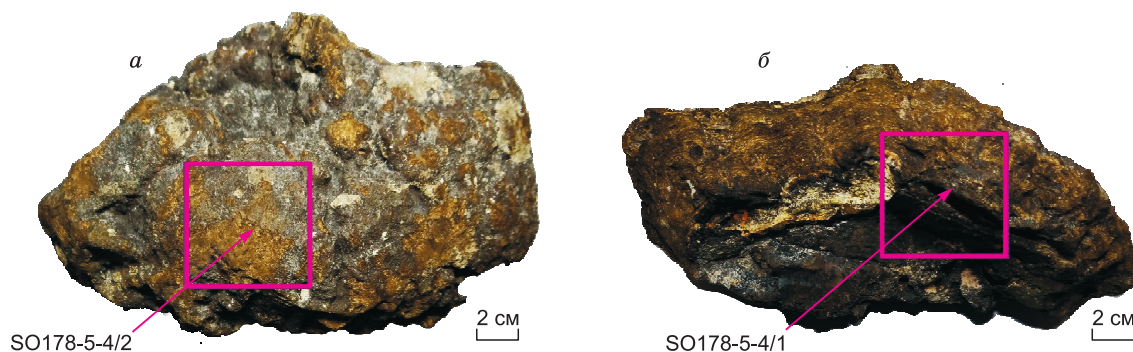


Fig. 5. Ferromanganese crust samples from the Sonne Ridge with sampling locations. *a*, Plan view; *b*, side view.

Table 1. Chemical composition of ferromanganese crusts from the Sonne Ridge compared to ferromanganese crusts of the World Ocean

Element	Samples from the Sonne Ridge		Hydrothermal crusts of the Sea of Japan		World Ocean, crusts from seamounts and uplifts	
	SO178-5-4/1	SO178-5-4/2	I	II	III	IV
Major elements, %						
Si	4.05	11.9	1.76	2.99	4.11	3.08
Ti	0.63	0.31	0.03	0.02	0.97	0.54
Al	0.99	2.11	0.62	0.77	1.12	0.48
Fe	13.6	16.1	2.84	2.10	15.1	0.60
Mn	29.6	17.9	50.0	48.7	19.0	44.5
Mg	1.52	0.98	1.40	0.99	1.16	1.88
Ca	2.24	1.83	1.26	0.91	3.79	1.77
Na	2.68	2.15	1.88	1.50	1.43	2.31
K	0.68	0.94	1.03	0.85	0.90	0.83
P	0.37	0.42	0.05	0.05	1.22	0.17
Mn/Fe	2.18	1.11	45.2	143	1.26	74.1
(Mn + Fe)/Ti	68.6	110	3173	4466	35.1	83.4
Trace elements, ppm						
Li	b.d.l.	2.44	343	309	100	1500
Be	2.33	3.39	0.33	0.35	4.73	0.4
Sc	7.21	11.1	1.51	1.32	12.5	67
V	528	527	609	171	700	202
Cr	25.8	14.6	8.98	16.4	100	41
Co	1801	684	361	367	5400	38
Ni	9120	3272	871	289	4100	344
Cu	616	416	120	60.1	1100	128
Zn	831	566	230	189	600	306
Ga	8.84	6.94	–	–	16.3	–
As	209	214	51.4	41.1	200	52
Rb	9.53	18.1	14.4	12.2	24.6	80
Sr	1305	1205	1900	1415	1300	595
Zr	364	437	15.8	11.5	–	–
Nb	58.8	22.7	1.17	1.12	–	–
Mo	579	462	251	250	400	582
Cd	8.60	7.19	3.25	2.12	3.87	7.8
Cs	0.49	0.86	0.59	0.60	2.97	3
Ba	1334	1285	13375	4411	1400	2419
Hf	7.19	6.70	0.28	0.27	–	–
Ta	1.05	1.04	0.07	0.17	–	–
W	87.7	59.0	95.2	36.8	–	–
Tl	211	84.2	4.20	3.33	99.1	–
Pb	445	618	13.5	6.42	1300	52
Th	44.4	43.3	0.78	0.72	20.03	0.44
U	9.64	9.22	11.2	10.1	11.1	1.98
REY, ppm						
Y	137	150	13.68	14.14	178	58
La	187	205	11.1	9.21	295	30.1
Ce	817	747	27.1	16.7	898	16.0
Pr	45.3	53.8	2.36	1.75	62	7.28
Nd	187	225	10.2	7.27	240	29.0

(continued on next page)

Table 1 (continued)

Element	Samples from the Sonne Ridge		Hydrothermal crusts of the Sea of Japan		World Ocean, crusts from seamounts and uplifts	
	SO178-5-4/1	SO178-5-4/2	I	II	III	IV
Sm	45.6	54.5	2.10	1.40	52	6.88
Eu	10.7	12.3	0.55	0.36	13	1.72
Gd	47.6	54.8	2.42	1.71	66	7.69
Tb	7.33	8.53	0.39	0.29	9	1.25
Dy	41.6	45.5	2.40	1.94	59	7.55
Ho	8.17	9.25	0.49	0.44	13	1.55
Er	22.3	24.6	1.45	1.45	37	4.32
Tm	3.31	3.54	0.20	0.22	5	0.66
Yb	23.2	23.2	1.41	1.54	37	4.29
Lu	3.37	3.32	0.20	0.25	6	0.70
∑REY	1587	1621	76.00	58.6	1770	213
Y/Ho	16.8	16.3	28.8	33.0	13.7	37.0
(Ce/Pr) _{PAAS}	2.00	1.54	1.27	1.06	1.61	0.24
(Eu/Eu*) _{PAAS}	1.08	1.06	1.13	1.08	1.02	1.10

Note. I, Belyaevsky Volcano, averaged data after (Mikhailik, 2014a); II, Medvedev Rise, averaged data after (Mikhailik, 2014a); III, hydrogenous crusts, data after (Baturin, 1993; Anikeeva et al., 2002; Melnikov, 2005), IV, hydrothermal crusts, data after (Baturin, 1993; Usui et al., 1997); b.d.l., below detection limit; dash, data unavailable.

Table 2. Major elements distribution in four mineral phases of ferromanganese crusts from the Sonne Ridge, ppm and %

Element	SO178-5-4/1, ppm					SO178-5-4/1, %					
	Phase I	Phase II	Phase III	Phase IV	∑ ph I, II, III, IV	Bulk	Phase I	Phase II	Phase III	Phase IV	∑
Si	755	1420	619	37,683	40,477	40,477	1.87	3.51	1.53	93.10	100
Ti	0.35	39	4982	244	5265	6300	0.01	0.74	94.62	4.64	100
Al	15.6	568	3380	4801	8764	9948	0.18	6.48	38.56	54.78	100
Fe	8.28	32,810	95,496	1693	130,007	135,800	0.01	25.24	73.45	1.30	100
Mn	141	282,899	1816	36	284,891	296,333	0.05	99.30	0.64	0.01	100
Mg	8249	3446	156	547	12,397	15,210	66.54	27.80	1.25	4.41	100
Ca	13,450	5061	25.4	708	19,244	22,350	69.89	26.30	0.13	3.68	100
Na	–	18,258	<1	1464	19,722	26,754	–	92.58	b.d.l.	7.42	100
K	3429	2084	10.2	1423	6947	6756	49.36	30.01	0.15	20.49	100
P	13.9	132	3369	19	3533	3725	0.39	3.74	95.35	0.52	100
Element	SO178-5-4/2, ppm					SO178-5-4/2, %					
	Phase I	Phase II	Phase III	Phase IV	∑ ph I, II, III, IV	Bulk	Phase I	Phase II	Phase III	Phase IV	∑
Si	910	2060	661	115,416	119,047	119,047	0.76	1.73	0.55	96.95	100
Ti	0.11	10	2007	375	2393	3100	0.00	0.42	83.90	15.68	100
Al	7.95	560	2760	14,613	17,941	21,100	0.04	3.12	15.38	81.45	100
Fe	7.10	31,760	113,888	3674	149,330	161,200	0.00	21.27	76.27	2.46	100
Mn	143	170,793	2778	56	173,771	178,667	0.08	98.29	1.60	0.03	100
Mg	4998	2040	263	1133	8434	9775	59.26	24.19	3.12	13.43	100
Ca	10,126	3683	41.7	2509	16,361	18,250	61.89	22.51	0.26	15.34	100
Na	–	12,648	<1	5068	17,716	21,453	–	71.39	b.d.l.	28.61	100
K	4023	760	15.9	3904	8702	9439	46.23	8.73	0.18	44.86	100
P	20.5	136	3612	35	3804	4183	0.54	3.58	94.97	0.91	100

Note. Dash means that the data are unavailable due to inability to determine Na as a result of leaching using the acetate buffer.

Table 3. Trace element distribution in four mineral phases of ferromanganese crusts from Sonne Ridge, ppm

Element	SO178-5-4/1						SO178-5-4/2					
	Phase I	Phase II	Phase III	Phase IV	Σ ph I, II, III, IV	Bulk	Phase I	Phase II	Phase III	Phase IV	Σ ph I, II, III, IV	Bulk
Li	1.99	b.d.l.	0.18	b.d.l.	2.17	b.d.l.	3.44	b.d.l.	0.42	b.d.l.	3.86	2.44
Be	0.06	0.53	1.28	0.11	1.97	2.33	0.08	0.94	1.87	0.29	3.17	3.39
Sc	0.12	0.018	5.99	0.75	6.87	7.21	0.17	b.d.l.	9.47	1.75	11.4	11.1
V	0.095	435	83.9	5.38	525	529	0.12	414	106	10.6	531	527
Cr	b.d.l.	0.009	1.69	2.61	4.31	25.8	b.d.l.	0.02	5.35	5.91	11.3	14.6
Co	0.040	1655	95.0	0.91	1752	1802	0.034	552	28.5	1.21	582	684
Ni	0.036	1490	85.5	3.39	1579	9120	29.5	524	27.0	4.55	586	3272
Cu	14.4	253	269	3.55	541	617	14.9	152	182	4.38	353	416
Zn	41.1	744	66.0	4.87	856	831	26.4	335	81.8	8.28	451	566
Ga	0.046	4.64	1.73	4.46	10.9	8.84	0.059	5.36	1.73	4.58	11.8	6.94
As	0.31	1.93	202	1.68	206	209	0.33	2.11	209	1.68	213	214
Rb	0.96	1.21	0.079	6.15	8.40	9.53	0.715	0.71	0.137	15.6	17.1	18.1
Sr	437	875	2.86	15.3	1329	1305	461	732	4.28	62.1	1260	1205
Zr	0.048	0.33	355	3.01	358	364	0.047	1.02	438	8.69	448	436
Nb	0.005	0.091	63.4	0.51	64.0	58.8	0.001	0.051	18.6	0.94	19.6	22.7
Mo	0.097	28.5	567	0.57	596	579	0.24	14.7	472	0.86	489	462
Cd	0.62	6.58	0.565	0.095	7.86	8.60	0.76	4.28	0.620	0.013	5.68	7.19
Cs	0.003	0.012	0.006	0.32	0.34	0.49	0.002	0.025	0.012	0.74	0.78	0.86
Ba	b.d.l.	1216	39.1	37.6	1293	1334	b.d.l.	1153	74.2	108	1335	1285
Hf	0.004	0.037	6.16	0.113	6.31	7.19	0.001	0.076	5.61	0.23	5.91	6.70
Ta	0.001	0.011	0.092	0.047	0.15	1.05	b.d.l.	0.013	b.d.l.	0.068	0.08	1.04
W	0.01	0.10	78.8	1.67	80.6	87.7	b.d.l.	0.16	53.5	0.27	53.9	59.0
Tl	6.45	188	2.28	0.37	197	211	14.2	60.0	1.48	0.45	76.1	84.2
Pb	0.06	32.9	387	8.04	429	445	0.01	80.8	485	6.03	572	618
Th	0.02	0.03	35.7	1.63	37.4	44.4	0.03	0.10	31.7	1.05	32.9	43.3
U	1.30	0.70	5.97	0.063	8.04	9.64	2.61	0.55	4.64	0.13	7.94	9.22

Total REY contents for samples SO178-5-4/1 and SO178-5-4/2 are 1587 and 1621 ppm, respectively (Table 1). Ce and Eu anomalies are positive and typical for hydrogenous ferromanganese crusts (Dubinin, 2006).

The results of studying Fe–Mn crusts using sequential leaching are presented in Tables 2, 3, and 4.

Phase I (easily leachable cations and carbonates) includes about 2/3 of the total Ca content (69.89 and 61.89% for samples SO178-5-4/1 and SO178-5-4/2, respectively). Mn, Fe, Si, and Al contents amount to thousandths and hundredths of a percent with respect to their total contents in samples (Table 2).

Phase II (elements associated with Mn oxides) includes the major amount of Mn (99.3 and 98.29% for samples SO178-5-4/1 and SO178-5-4/2, respectively), as well as 26.3% (SO178-5-4/1) and 22.51% (SO178-5-4/2) of the total Ca content (Table 2). Fe, Si, and Al are present in minor amounts comparable to the values for the first phase. High Ca content in the manganese phase is due to inclusion of this element into crystalline lattices of minerals forming the ferromanganese crusts of the Sea of Okhotsk (Chukhrov et al., 1989).

Phase III (elements associated with Fe oxide-hydroxides) is characterized by Fe release of 73.45% (SO178-5-4/1) and 76.27% (SO178-5-4/2).

Phase IV (residual aluminosilicate) includes the major amounts of Si and Al: SO178-5-4/1—93 and 54.78%; SO178-5-4/2—96.6 and 81.45% (Table 2). The remaining elements are present in minor quantities, however, K and Ca contents are quite high, which may be attributed to specific features of the allothigenic impurity.

REY contents by mineral phases in numeric and percentage forms are presented in Table 4 and Fig. 6.

REY content in Phase I does not exceed 2.62–3.13% (total REY content as a percentage from the bulk amount), with the minimum values for Ce at 0.05–0.06% and maximum values for Y at 4.61–5.67%. Here, the highest contents are observed for medium REY contents, with Gd showing the maximum at 3.91–4.57 (Table 4).

Phase II includes the highest amount of REY with maximum La accumulation up to 72.11% (SO178-5-4/1) and 78.63% (SO178-5-4/2). Although some elements in sample SO178-5-4/1 show maximum concentrations in other extracts, while SO178-5-4/2 is characterized by total domi-

Table 4. Rare earth elements and Y contents in four mineral phases of ferromanganese crusts from the Sonne Ridge, ppm and %

Element	SO178-5-4/1, ppm						SO178-5-4/1, %			
	Phase I	Phase II	Phase III	Phase IV	Σ ph I, II, III, IV	Bulk	Phase I	Phase II	Phase III	Phase IV
Y	5.56	67.6	33.0	14.3	120	137	4.61	56.08	27.41	11.90
La	2.51	126	12.2	34.2	175	187	1.43	72.11	6.96	19.49
Ce	0.44	480	108	222	811	817	0.05	59.20	13.34	27.41
Pr	0.63	18.9	5.28	13.7	38.5	45.3	1.62	49.19	13.72	35.47
Nd	3.48	71.6	22.3	61.7	159	187	2.19	45.03	14.03	38.76
Sm	1.12	13.2	6.57	16.7	37.6	45.6	2.99	35.08	17.50	44.43
Eu	0.29	2.97	1.66	3.74	8.67	10.7	3.32	34.29	19.20	43.20
Gd	1.48	15.2	7.42	13.7	37.8	47.5	3.91	40.30	19.62	36.16
Tb	0.19	2.38	1.49	1.93	6.00	7.33	3.24	39.66	24.90	32.20
Dy	1.09	13.5	10.5	8.89	34.0	41.6	3.19	39.81	30.85	26.14
Ho	0.22	2.82	2.36	1.37	6.77	8.17	3.30	41.63	34.87	20.21
Er	0.57	7.99	7.95	3.01	19.5	22.3	2.91	40.93	40.72	15.44
Tm	0.056	1.05	1.37	0.31	2.79	3.31	2.02	37.51	49.31	11.17
Yb	0.38	6.07	9.74	1.60	17.8	23.2	2.14	34.11	54.76	8.99
Lu	0.06	0.91	1.49	0.22	2.67	3.37	2.35	33.84	55.75	8.06
Σ , %	–	–	–	–	–	–	2.62	43.92	28.20	25.27

Element	SO178-5-4/2, ppm						SO178-5-4/2, %			
	Phase I	Phase II	Phase III	Phase IV	Σ ph I, II, III, IV	Bulk	Phase I	Phase II	Phase III	Phase IV
Y	7.78	96.0	27.6	5.88	137	150	5.67	69.95	20.10	4.28
La	3.25	154	20.4	18.2	196	205	1.66	78.63	10.42	9.29
Ce	0.49	550	151	109	811	747	0.06	67.84	18.65	13.45
Pr	0.91	30.3	9.63	9.20	50.0	53.8	1.81	60.56	19.24	18.39
Nd	5.08	117	42.3	42.2	207	225	2.46	56.63	20.46	20.45
Sm	1.69	23.6	12.2	11.4	48.8	54.5	3.45	48.39	24.89	23.27
Eu	0.42	5.28	2.91	2.44	11.1	12.3	3.80	47.78	26.34	22.09
Gd	2.16	25.2	11.7	8.24	47.3	54.8	4.57	53.35	24.66	17.42
Tb	0.28	3.97	1.93	0.99	7.17	8.53	3.88	55.31	26.95	13.86
Dy	1.54	22.2	11.7	4.16	39.6	45.5	3.89	55.95	29.65	10.51
Ho	0.30	4.55	2.29	0.57	7.71	9.25	3.92	59.02	29.71	7.35
Er	0.74	12.4	6.95	1.20	21.3	24.6	3.48	58.26	32.65	5.61
Tm	0.08	1.63	1.09	0.12	2.92	3.54	2.77	55.96	37.31	3.96
Yb	0.49	10.0	7.48	0.59	18.6	23.2	2.64	53.89	40.30	3.17
Lu	0.08	1.47	1.10	0.08	2.73	3.32	2.90	53.68	40.35	3.06
Σ , %	–	–	–	–	–	–	3.13	58.35	26.78	11.74

Note. Maximum content of an element in one of four phases is shown in boldface.

nance of the whole spectrum of REY in this phase. This distribution indicates differences in hydrochemical parameters of seawater during formation of the lower and the upper layers of the crusts (Khanchuk et al., 2015). Total REY content for Phase II is 43.92 and 58.35% for samples SO178-5-4/1 and SO178-5-4/2, respectively.

Phase III is characterized by moderate lanthanide and Y accumulation, with the maximum values displayed by heavy elements. Total REY contents with respect to bulk amounts are 28.20 and 26.78% for samples SO178-5-4/1 and SO178-5-4/2, respectively.

Residual aluminosilicate phase IV concentrates a rather large amount of REY, with the total content reaching 25.27 and 11.74% for samples SO178-5-4/1 and SO178-5-4/2. Here, concentrations of medium elements are significantly higher, than those of light and heavy ones. High REY content in the aluminosilicate phase depends to a greater extent on remoteness of the recovered sample from the continent. For example, FMD in central areas of the Pacific (Bau and Koschinsky, 2009) and Indian Oceans (Prakash et al., 2012) display the lowest REY contents in the residual phase, which grow at shorter distances from the continent, as noted

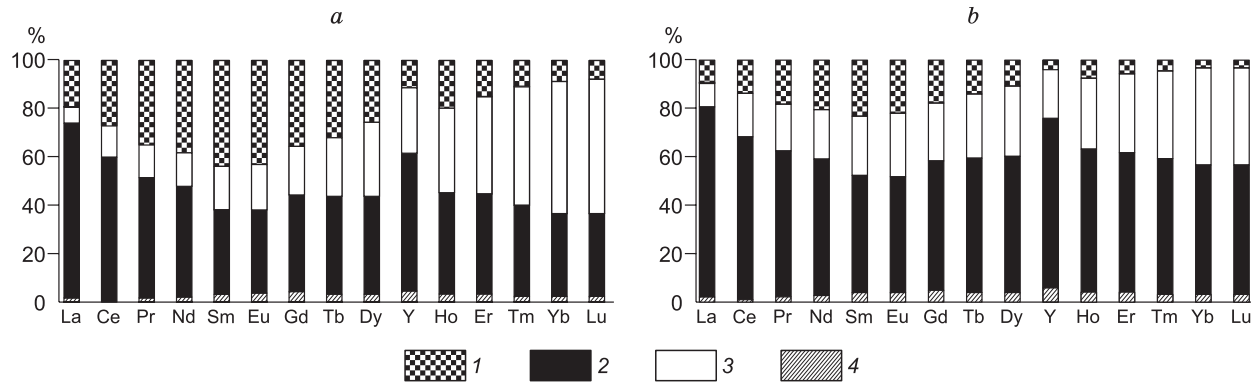


Fig. 6. REY percentages in mineral phases of the ferromanganese crusts from the Sonne Ridge. 1, Phase I (easily leachable cations and carbonates); 2, Phase II (Mn oxides); 3, Phase III (Fe oxide-hydroxides); 4, Phase IV (residual); a, sample SO178-5-4/1, b, sample SO178-5-4/2.

in course of investigation of the crusts of the Detroit Guyot (Emperor seamount chain) (Khanchuk et al., 2015).

DISCUSSION

Ferromanganese crusts from the Sonne Ridge are very similar in their texture, structure, and chemical composition to hydrogenous ferromanganese crusts from seamounts in the central part of the Sea of Okhotsk (Mikhailik et al., 2009) and guyots of Magellan and Marcus-Wake seamount clusters (Melnikov, 2005), while being significantly different from various hydrothermal rocks of the Kuril Island Arc (Anikeeva et al., 2008).

Vernadite composition of the studied crusts matches the mineralogy of the Fe–Mn crusts from Magellan and Marcus-Wake guyots, which are currently the most researched in the Pacific Ocean (Andreev and Anikeeva, 1993; Anikeeva et al., 2002; Melnikov, 2005), as well as nodules from basins in the Pacific and Indian Oceans (Murdmaa and Skornyakova, 1986; Skornyakova et al., 1989), and hydrogenous crusts of the Kashevarov Trough (Mikhailik et al., 2009). At the same time, diagenetic nodules of the pelagic oceanic zones are comprised of 10Å manganite (with prevalence of asbolane-buserite) with vernadite impurity, and hydrothermal ferromanganese deposits are formed by 7Å (birnessite) and 10Å (todorokite) manganites, as well as pyrolusite (Usui et al., 1986; Mikhailik et al., 2004, 2014a; Glasby et al., 2006; Mikhailik, 2007). Thus, the mineral composition of ferromanganese crusts of the Sonne Ridge matches the hydrogenous FMD of the World Ocean.

Ferromanganese crusts from the Sonne Ridge occupy the area near the boundary of hydrothermal deposits (Fig. 7) in the ternary plot (Fe/Mn/(Ni + Cu + Co) × 10) (Bonatti et al., 1972). The field of explicitly hydrothermal deposits from different areas (Hein et al., 1996; Usui et al., 1997; Mikhailik et al., 2004; Glasby et al., 2006) includes inherently hydrogenous Fe–Mn deposits from the Baltic, Okhotsk, Laptev, and Black seas, as well as freshwater lakes (Strakhov et al., 1968; Kalyagin et al., 2001; Astakhova and Satarova, 2005).

Thus, contents of the main metals in ferromanganese crusts of marginal seas do not provide an unambiguous answer regarding their origin, and locations of their respective values in Bonatti’s diagrams are not as persuasive, compared to the open part of the ocean (Kronen, 1982). Moreover, the diagram most likely characterizes growth rates of Fe–Mn deposits (Bazilevskaya, 2009).

Pb, Zn, V, and Mo may formally be considered among the main ore elements of the crusts (Baturin, 1993). Their

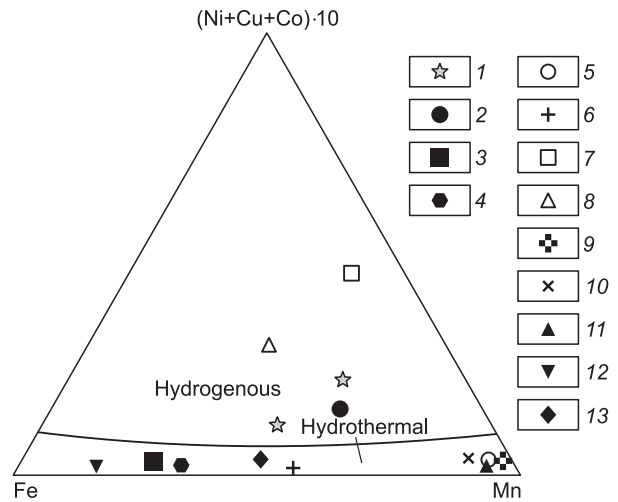


Fig. 7. Different genetic types of ferromanganese deposits on the ternary diagram (Fe/Mn/(Ni + Cu + Co) × 10) after (Bonatti et al., 1972). 1, Fe–Mn crusts from the Sea of Okhotsk, Sonne Ridge (present paper); 2, Fe–Mn crusts from the Sea of Okhotsk (Mikhailik et al., 2009); 3, Fe–Mn deposits from the Laptev Sea (Kalyagin et al., 2001); 4, Fe–Mn deposits from the Baltic Sea (Strakhov et al., 1968); 5, hydrothermal Fe–Mn crusts from the Sea of Japan (Mikhailik et al., 2014a); 6, Fe–Mn deposits from the Punson–Yarvi lake (Strakhov et al., 1968); 7, Fe–Mn nodules from the Clarion–Clipperton Zone (Anikeeva et al., 2002); 8, cobalt-rich Fe–Mn crusts from seamounts and uplifts (Anikeeva et al., 2002); 9, hydrothermal Fe–Mn crusts from “hot spots” (Hein et al., 1996); 10, Fe–Mn deposits from mid-oceanic ridges (Usui et al., 1997); 11, Fe–Mn crusts from island arc volcanoes (Glasby et al., 2006); 12, Fe–Mn nodules from the Black Sea (Strakhov et al., 1968); 13, Fe–Mn deposits from the central part of the Sea of Okhotsk (Astakhova and Satarova, 2005).

contents in the studied crusts for samples SO178-5-4/1 and SO178-5-4/2 were as follows (ppm): Pb—9.53 and 18.1; Zn—831 and 566; V—528 and 527; Mo—579 and 462 (Table 1). Average contents of these elements in hydrogenic crusts of the Pacific Ocean are as follows (ppm): Pb—700; Zn—900; V—400; Mo—400 (Andreev, 1994). Mo contents in crusts of the Sea of Okhotsk is close to its average content in abyssal nodules (400 ppm) and crusts of guyots (500 ppm) (Anikeeva et al., 2002).

The group of nonmetallic major elements includes Al, alkaline elements Li, Na, K, Rb, and Cs, and alkaline-earth metals Ca, Sr, Ba, Ra, and P (Baturin, 1993). Ca content in the studied crusts is 2.24 and 1.83%. Ca content in ferromanganese crusts of the World Ocean is slightly higher, namely 3.79%. The crusts of the Sonne Ridge are close in Na, Al, Mg, K, and P contents to nonphosphatized Fe–Mn crusts from underwater seamounts and elevations of the World Ocean (Table 1). The contents of Sr (0.13 and 0.12%) and Ba (0.133 and 0.128%) are approximately equal to those in hydrogenous formations of the Pacific Ocean (Sr—0.13%; Ba—0.14%). Contents of these elements in hydrothermal ferromanganese crusts are significantly higher (Hein et al., 1987, 1996; Mikhailik et al., 2004). In terms of average phosphorus content, ferromanganese crusts from the Sonne Ridge are most similar to nodules from abyssal basins, the values being 0.39 and 0.24%, respectively. Phosphorus contents are significantly higher in phosphatized layers of cobalt-rich guyot crusts (1.23%), while the average value for hydrothermal crusts is 1.06% (Anikeeva et al., 2002).

Contents of trace elements (Be, Sc, Rb, Cs, Se, Cr, As, Ge, Br, I, Cd, Sb, Tl, In, Hg, Bi, Th, and U) in the studied formations (Table 1) are close to those in hydrothermal crusts from various regions of the World Ocean (Baturin, 1993; Andreev, 1994; Anikeeva et al., 2002). Li contents are rather low, which is typical for hydrogenous crusts, whereas its contents rise sharply in hydrothermal differences reaching 1500 ppm (Strakhov et al., 1968; Baturin, 1993).

In terms of chemical properties, the REY group, which is very sensitive to physicochemical changes in the environment and applicable for identifying the genesis of rocks, is of greatest interest. To understand REY composition changes in the environments, the effect of differences in their abundance needs to be eliminated. It is achieved by normalization of the studied REY compositions by the REY composition in chondrites or shales (Dubinin, 2006). REY content, as well as Ce and Eu anomaly sizes and Y/Ho relations, are presented in Table 1. These values are presented in a more illustrative fashion in Fig. 8, which shows the comparative distribution of REY for the crust samples from the Sonne Ridge and ferromanganese crusts of various genesis.

Two peaks can be clearly seen in these plots: the positive peak for the Ce anomaly and the negative peak for the Y anomaly. A positive Ce anomaly is main attributes of hydrothermal genesis for ferromanganese crusts. It is confirmed by $(\text{Ce}/\text{Pr})_{\text{PAAS}}$ relation (PAAS subscript indicates the normalization by Post Archean Australian Shale), whose value

is typically more than 1. The values of $(\text{Ce}/\text{Pr})_{\text{PAAS}}$ for the analyzed crusts are 1.54 and 2.00 (Table 1). The presence of a positive Ce anomaly is explained by oxidation of Ce in seawater by oxide-hydroxides (Bau et al., 1996; Mills et al., 2001). A negative Ce anomaly is typical for hydrothermal FMD of mid-oceanic ridges, island arc systems, and “hot spots”, as well as fast-growing diagenetic concretions under suboxidative conditions (Usui et al., 1997).

The studied samples are characterized by slightly manifested positive Eu anomalies with values 1.08 and 1.06 (Table 1); these are calculated as follows: $(\text{Eu}/\text{Eu}^*)_{\text{PAAS}} = \text{Eu}/\text{Eu}_{\text{PAAS}} / (1/2 \cdot \text{Sm}/\text{Sm}_{\text{PAAS}} + 1/2 \cdot \text{Gd}/\text{Gd}_{\text{PAAS}})$ (Dubinin, 2006). The value of $(\text{Eu}/\text{Eu}^*)_{\text{PAAS}}$ being more than 1 is typical for hydrogenous ferromanganese crusts in various regions of the Pacific Ocean, where it varies from 1.11 to 1.29 (Bau et al., 1996). The Eu anomaly is, in turn, observed in low-temperature hydrothermal FMD (Usui et al., 1997; Mills et al., 2001).

A negative Y anomaly is observed in all nonphosphatized ($P < 0.7\%$) (Koscinsky et al., 1997) ferromanganese crusts of the Pacific Ocean. It is calculated based on Y/Ho relation as follows: the anomaly is considered positive if its value is above 28, and negative otherwise (Bau and Dulski, 1995). The value of this relation for the Pacific is below 28 and on average equals 17 for guyot crusts in the northern part of the Pacific Ocean and 22 in the south (Bau et al., 1996). Phosphorus contents in the studied ferromanganese crusts of the Sea of Okhotsk are 0.37 and 0.42%, and Y/Ho values are 16.8 and 16.3, respectively. Hydrothermal manganese crusts display a positive Y anomaly with the value above 28 ($\text{Y}/\text{Ho} > 28$) (Usui et al., 1997).

Thus, the crusts of the Sonne Ridge may be classified as hydrogenous based on bulk REY distribution, which is reflected in Fig. 8.

However, the REY distribution data for hydrothermal ferromanganese crusts of the Sea of Japan showed that they are mostly attributed to the hydrogenous and terrigenous components, while the endogenous component (which is superior in volume) is “depersonalized” in the total ore mass (Mikhailik et al., 2014a, 2017). Essentially, the bulk REY composition (ferroan and aluminosilicate phases) in these samples does not reflect the hydrothermal supply, and only summarizes the eventual effects of hydrogenous and exogenous processes. The endogenous part is reflected by REY of the manganese phase, whose contents are negligibly small, with contents of some elements below the detection limit, and do not influence the total content. To trace the influence of the hydrothermal component on formation of ferromanganese crust compositions, we analyzed REY distributions in mineral phases of the ferromanganese crusts of the Sonne Ridge.

Rare earths in the FMD do not have their inherent mineral phases, as they are sorbed by intergrown Fe and Mn oxide-hydroxides (Dubinin, 2006). Aluminosilicate phases in some regions may accumulate significant amounts of these elements (Khanchuk et al., 2015). Highly mobile

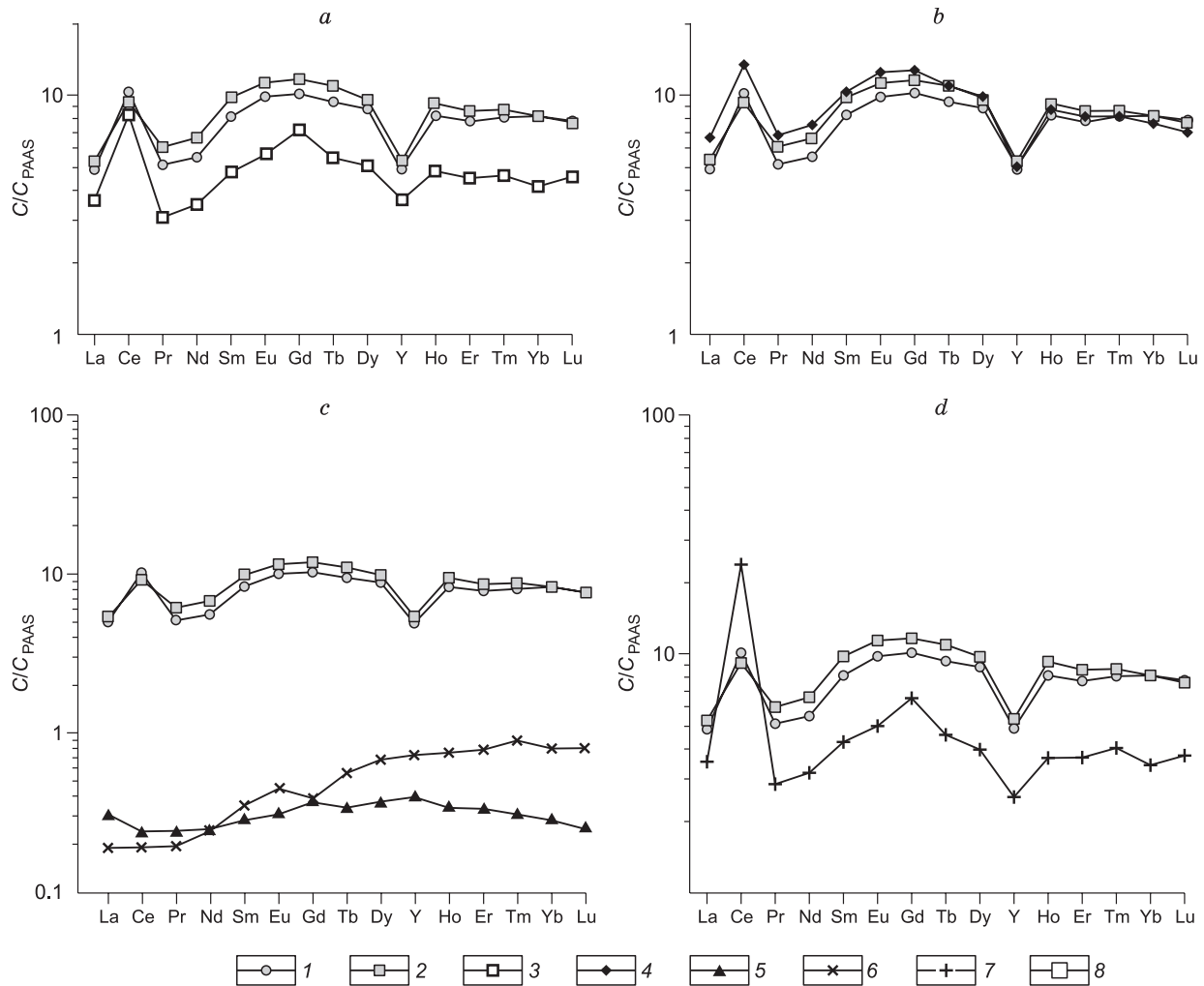


Fig. 8. Shale-normalized REY patterns distribution (bulk contents) in ferromanganese crusts from the Sonne Ridge compared to FMD of various origins. 1, sample SO178-5-4/1; 2, sample SO178-5-4/2; 3, hydrogenous Fe–Mn crusts from the Andaman Sea (Prakash et al., 2012); 4, hydrogenous Fe–Mn crusts from the Detroit Guyot (Khanchuk et al., 2015); 5, hydrothermal Fe–Mn crusts from the Sea of Japan (Mikhailik et al., 2014b); 6, hydrothermal Fe–Mn crusts from the Andaman Sea (Prakash et al., 2012); 7, Fe–Mn nodules from the Mid-Indian basin (Prakash et al., 2012); 8, hydrogenous Fe–Mn crusts of the Line Islands (Bau and Koschinsky, 2009). *a*, FMD from back-arc basins; *b*, FMD from the open parts of the Pacific Ocean; *c*, FMD from marginal seas; *d*, FMD from the central parts of the Indian and Pacific Oceans.

forms of REY (Phase I) in FMD of various origins are concentrated in subordinate quantities (Bau and Koschinsky, 2009; Jiang et al., 2011; Prakash et al., 2012).

The distribution of shale-normalized (PAAS, after McLennan, 1989) Phase-I REY patterns of the ferromanganese crusts of the Sonne Ridge (Fig. 9A) is close to their distribution in hydrogenous and hydrothermal crusts in various parts of the World Ocean. This similarity between REY distribution plots for ferromanganese crusts of various genesis is explained by the common fractionation mechanism of highly mobile forms of REY by carbonate components of FMD from various regions of the World Ocean. A negative Ce anomaly indicates the oxide settings, since the presence of a positive Ce anomaly during the recovery of highly mobile forms of REY indicates the reductive environment of sedimentation (Mikhailik et al., 2016).

A sharp difference in REY accumulation in the manganese phase is observed between the crusts of the Sonne Ridge and hydrothermal FMD of the Andaman Sea and the Sea of Japan (Fig. 9B, c) (Prakash et al., 2012; Mikhailik, 2014b). It is associated with different sources of the material that forms the manganese part and indicates no influence of the hydrothermal component, despite it being involved during the formation of the bulk composition of the crusts. In this phase, a lot of similarities in REY patterns are observed between the studied crusts and hydrogenous crusts of back-arc basins (Fig. 9B, a) and deepwater nodules (Prakash et al., 2012). The difference in REY patterns distribution is observed compared to the guyot crusts of the central Pacific (Fig. 9B, b) (Khanchuk et al., 2015). It can be seen from the figure that the curve reflecting the fractionation of elements

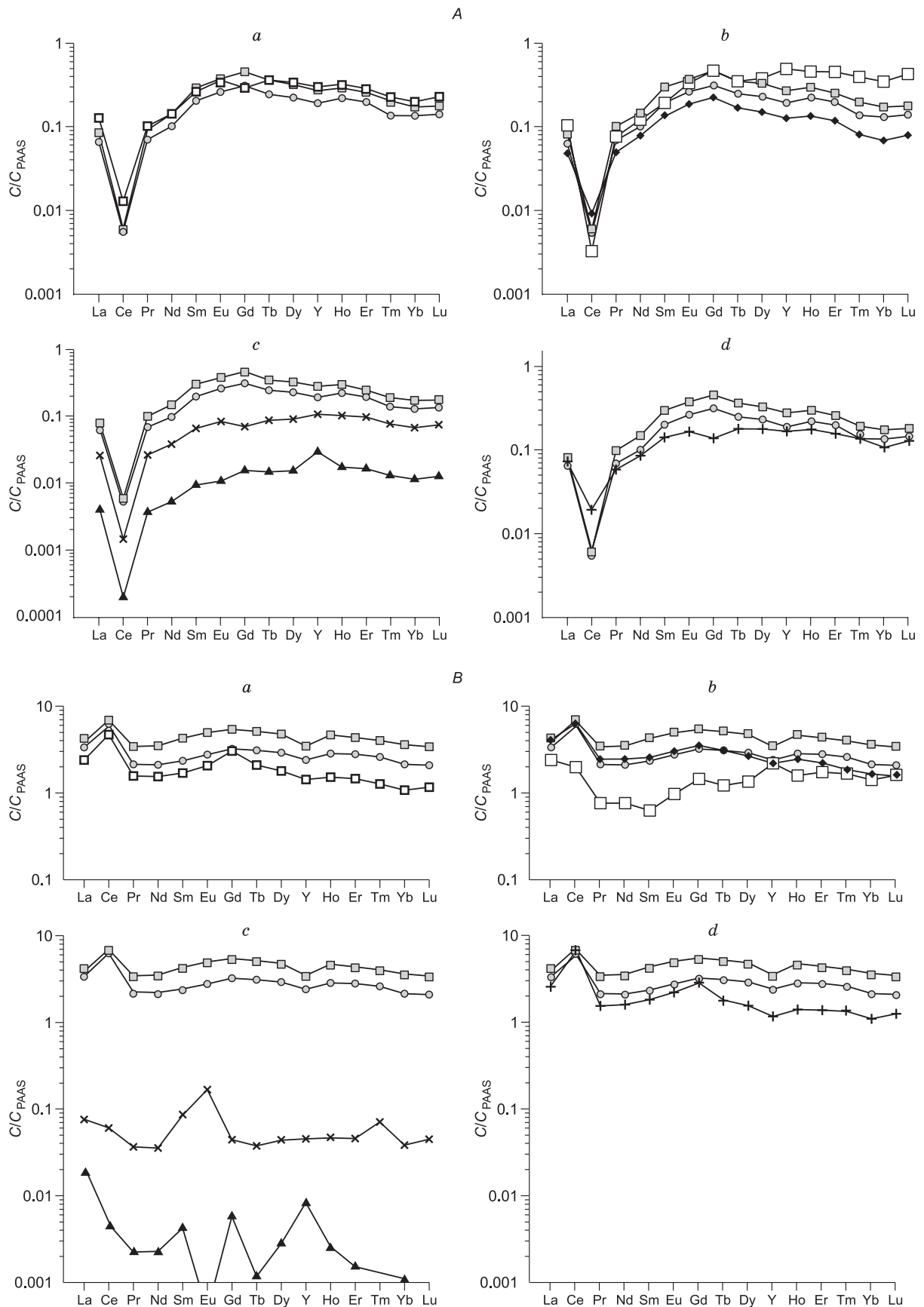


Fig. 9 (to be continued).

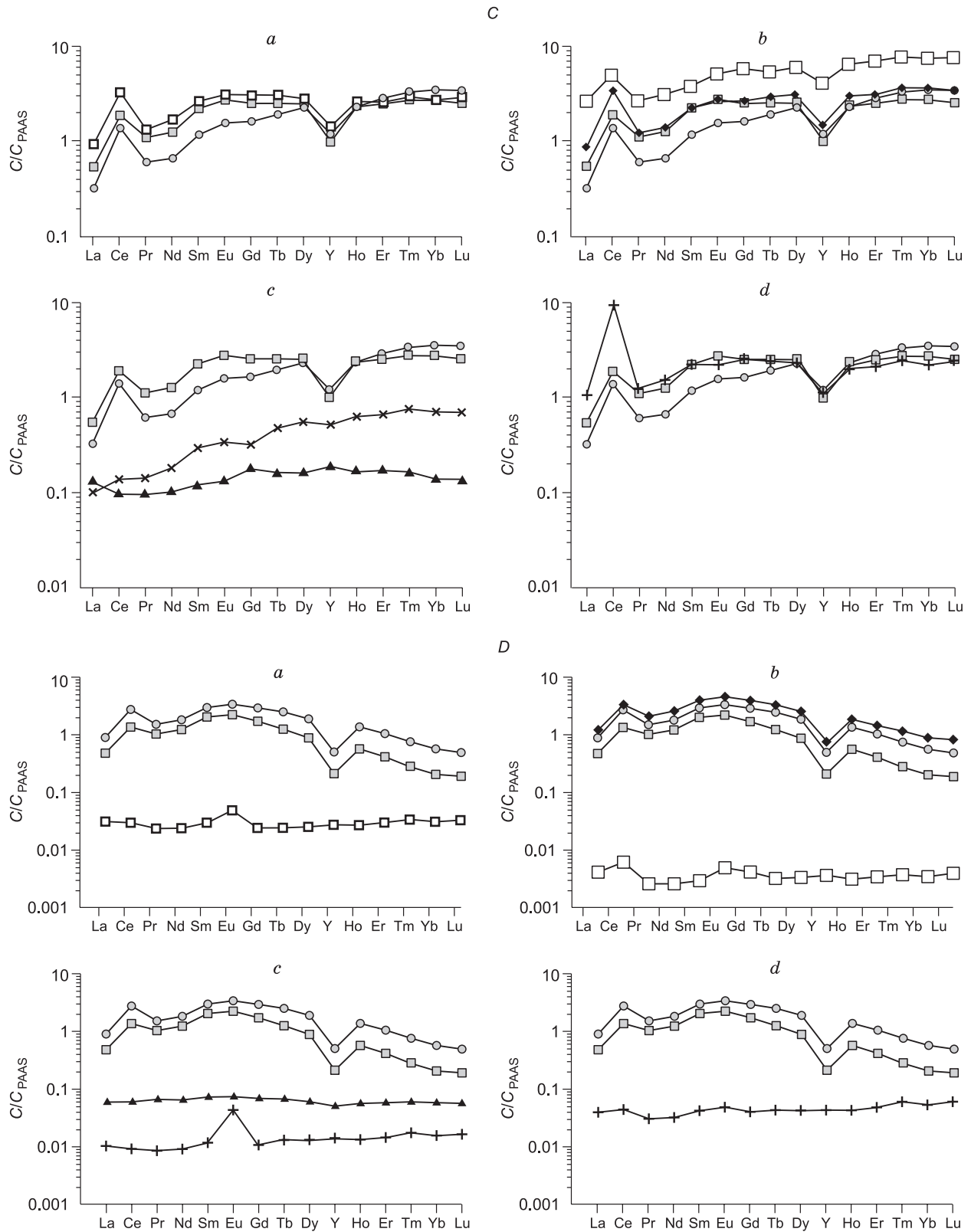


Fig. 9. Shale-normalized REY distribution for crust samples from the Sonne Ridge compared to samples of various origins. A–D, mineral phases I–IV, respectively. a–d, see Fig. 8.

in the crusts from Line Islands is slightly different but shows an overall similar trend.

Similarities in REY patterns distribution are found while comparing their trends in the ferrous phase with the FMD of hydrogenous origin in various geodynamic settings (Fig. 9C, *a, b, d*). Therefore, regardless of the geological conditions of their occurrence, REY are distributed in the ferrous phases of hydrogenous and diagenetic differences under the same scenario. REY patterns distribution in phase III is different for the hydrothermal crusts of back arc basins (Fig. 9C, *c*). In case of hydrothermal type, REY patterns distribution in this phase most likely reflects the REY composition of the neutral-buoyancy plume, which represents the main source of hydrothermal ferromanganese crusts. Here, hydrogenous REY composition is formed on Fe oxide-hydroxides. The prevalence of heavy REY over the light ones in them is most likely related to the time of the hydrothermal plume being exposed to seawater, as well as remoteness of the crusts being formed from the hydrothermal vent. As a result, REY composition of the ferroan phase becomes close to that of the background suspension of the hydrothermal field or the suspension of the neutral-buoyancy plume (Dubinin, 2006).

Distribution of REY patterns in residual aluminosilicate phases is different in all the studied regions (Fig. 9D), except for the crusts of the Detroit guyot, which indicates different rock compositions of the distributive province. REY fractionation in the crusts of the Sonne Ridge and hydrogenous crusts from the central part of the Sea of Okhotsk (Mikhailik et al., 2014c) and the northern part of the Pacific Ocean (Khanchuk et al., 2015) indicates the common source of the distributive province spreading over vast areas of the North Pacific. The aluminosilicate part of FMD of the Indian Ocean and the Central Pacific shows a different pattern, which indicates a different source rock composition, which generates an erratic supply in these regions of the World Ocean.

Thus, the presence of ferromanganese crusts on the slopes from the submarine Volcano 1 of the Sonne Ridge implied their hydrothermal genesis. However, morphology, structure, mineral and bulk chemical compositions indicated hydrogenous origin. Detailed investigation of distribution of the major elements and rare earth elements in mineral phase confirmed the hydrogenous genesis of the ferromanganese crusts from the Sonne Ridge. The studies performed are yet another proof that marine ferromanganese ore genesis is a very complex phenomenon, and that judgments on FMD genesis based on one or two attributes are not persuasive enough. A final conclusion may only be drawn following a deep detailed research of chemical composition using advanced methods, which the present study clearly confirms.

CONCLUSIONS

Ferromanganese deposits in the Pacific Ocean area have been rather well studied. At the same time, the information

on FMD in marginal seas is very poor, which makes research in this area a rather topical matter. Advanced analytical methods using phase analysis make it possible to obtain new data providing a detailed understanding of the genesis of marine ferromanganese deposits (Mikhailik et al., 2014a; Khanchuk et al., 2015). The necessity for introducing new research methods making it possible to identify the sources of the elements with high confidence is now obvious due to potential benefits they provide in terms of developing the general theory of the oceanic ferromanganese ore genesis and discovering specific features of metallogenic zoning of the Pacific Ocean floor and its periphery.

The analysis of factual information and the data from the literature have shown that ferromanganese crust samples from submarine volcanoes of the Sonne Ridge are deposited in ridge-top areas of the slopes and may preserve information on postvolcanic hydrothermal activity.

The study of textural and structural attributes of ferromanganese crusts from the Sonne Ridge shows their similarity to the hydrogenous Fe–Mn crusts from oceanic guyots.

Primarily vernadite mineral composition of the ferromanganese crusts from the Sonne Ridge is another piece of evidence in favor of their hydrogenous genesis since vernadite is the main mineral of hydrogenous oceanic Fe–Mn deposits.

In terms of concentrations of major and trace elements, ferromanganese crusts from the Sonne Ridge show contents of Mn, Fe, and the main trace elements close to those of hydrogenous crusts of seamounts and elevations of the Pacific Ocean. The interpretation of bulk and phase distributions of REY compositions provides convincing evidence of hydrogenous nature of the ferromanganese crusts from the Sonne Ridge.

Discovery of hydrogenous ferromanganese crusts with thicknesses of over 4 cm in the Sonne Ridge indicates the scale of mineralization in the Sea of Okhotsk. New data on metal distribution in mineral phases of the ferromanganese crusts may be used to refine the technology of industrial metal extraction.

The authors thank A.N. Derkachev, P.Ya. Tishchenko, and the employees of the Pacific Oceanological Institute of the Far Eastern Branch of the Russian Academy of Sciences for the provided rock material.

The work was supported by the Russian Foundation for Basic Research (project No. 18-05-00436A).

REFERENCES

- Andreev, S.I., 1994. Metallogeny of Ferromanganese Formations of the Pacific Ocean [in Russian]. Nedra, St. Petersburg.
- Andreev, S.I., Anikeeva, L.I., 1993. Types of oceanic oxide ferromanganese Ores, in: Cobalt-Bearing Ferromanganese Crusts of the Pacific Ocean [in Russian]. VNIIOkeangeologiya, St. Petersburg, VNIIOkeangeologiya, pp. 26–33.
- Andreev, S.I., Anikeeva, L.I., Alekseev, A.M., 2007. Mineral Resources of the World Ocean: Study and Development Concept (until the Year 2020) [in Russian]. VNIIOkeangeologiya, St. Petersburg.

- Anikeeva, L.I., Andreev, S.I., Kazakova, V.E., Aleksandrov, P.A., Zadorov, M.M., 2002. Cobalt-Rich Ores in the World Ocean [in Russian]. VNIIOkeangeologiya, St. Petersburg.
- Anikeeva, L.I., Kazakova, V.E., Gavrilenko, G.M., Rashidov, V.A., 2008. Ferromanganese crust formations of the West Pacific transition zone. *Vestnik KRAUNTs, Nauki o Zemle* 11 (1), 10–31.
- Astakhova, N.V., 2007. Authigenic Minerals of Late Cenozoic Sediments of East Asian Marginal Seas [in Russian]. *Dal'nauka, Vladivostok*.
- Astakhova, N.V., 2009. Precious and nonferrous metals in the ferromanganese crusts of the central Sea of Okhotsk. *Oceanology* 49 (3), 405–417.
- Astakhova, N.V., Sattarova, V.V., 2005. The geochemistry of ferromanganese formations in the Central Sea of Okhotsk. *Vulkanologiya i Seismologiya*, No. 3, 29–33.
- Baturin, G.N., 1993. *Oceanic Ores* [in Russian]. Nauka, Moscow.
- Baturin, G.N., Dubinchuk, V.T., Rashidov, V.A., 2012. Ferromanganese crusts from the Sea of Okhotsk. *Oceanology* 52 (1), 88–100.
- Bau, M., Dulski, P., 1995. Comparative study of yttrium and rare-earth elements behaviours in fluorine-rich hydrothermal fluids. *Contrib. Mineral. Petrol.* 119 (2–3), 213–223.
- Bau, M., Koschinsky, A., 2009. Oxidative scavenging of cerium on hydrous Fe oxide: Evidence from the distribution of rare earth elements and yttrium between Fe oxides and Mn oxides in hydrogenetic ferromanganese crusts. *Geochim. J.* 43 (1), 37–47.
- Bau, M., Koschinsky, A., Dulski, P., Hein, J.R., 1996. Comparison of the partitioning behaviors of yttrium, rare earth elements, and titanium between hydrogenetic marine ferromanganese crusts and seawater. *Geochim. Cosmochim. Acta* 60 (10), 1709–1725.
- Bazilevskaya, E.S., 2009. Ocean environment and developing of oceanic iron-manganese ores. *Dokl. Earth Sci.* 429 (2), 1417–1419.
- Bonatti, E., Kreamer, T., Rydell, H., 1972. Classification and genesis of submarine iron manganese deposits, in: Horn, D.R. (Ed.), *Ferromanganese Deposits on the Ocean Floor*. Office for the International Decade of Ocean Exploration, National Science Foundation, pp. 149–165.
- Chukhrov, F.V., Gorshkov, V.A., Drits, V.A., 1989. *Hypergenetic Manganese Oxides* [in Russian]. Nauka, Moscow.
- Dubinin, A.V., 2006. *Geochemistry of Rare Earth Elements in the Ocean* [in Russian]. Nauka, Moscow.
- Dullo, W.-Ch., Biebow, N., Georgeleit, K. (Eds.), 2004. SO178-KO-MEX Cruise Report: RV SONNE. Mass Exchange Processes and Balances in the Okhotsk Sea. Kiel.
- Gavrilenko, G.M., 1997. Submarine Volcanic and Hydrothermal Activity as a Source of Metals in Island-Arc Iron-Manganese Formations [in Russian]. *Dal'nauka, Vladivostok*.
- Gavrilenko, G.M., Khramov, S.V., 1986. Iron-manganese formations on the slopes of the Kuril Island Arc. *Vulkanologiya i Seismologiya*, No. 2, 97–100.
- Glasby, G.P., Cherkashev, G.A., Gavrilenko, G.M., Rashidov, V.A., Slovtsov, I.B., 2006. Submarine hydrothermal activity and mineralization on the Kurile and western Aleutian islands arcs, N.W. Pacific. *Mar. Geol.* 231 (1–4), 163–180.
- Haley, B.A., Klinkhammer, G.P., McManus, J., 2004. Rare earth elements in pore waters of marine sediments. *Geochim. Cosmochim. Acta* 68 (6), 1265–1279.
- Hein, J.R., Fleishman, C.L., Morgenson, L.A., Bloomer, S.H., Stern, R.J., 1987. Submarine ferromanganese deposits from the Mariana and Volcano volcanic arcs, West Pacific. *Open-File Rep.* 87–281. U.S. Geol. Surv.
- Hein, J.R., Gibbs, A.E., Clauge, D.A., Torresan, M., 1996. Hydrothermal mineralization along submarine rift zones, Hawaii. *Mar. Georesour. Geotechnol.* 14 (2), 177–203.
- Jiang, X.J., Lin, X.H., Yao, D., Guo, W.D., 2011. Enrichment mechanisms of rare earth elements in marine hydrogenic ferromanganese crusts. *Sci. China Earth Sci.* 54 (2), 197–203.
- Kalyagin, A.N., Tishchenko, P.Ya., Gukov, A.Yu., Volkova, T.I., Kurilko, L.N., Chichkin, R.V., 2001. The nature of the ferromanganese formations of the Laptev Sea. *Tikhookeanskaya Geologiya* 20 (2), 87–96.
- Khanchuk, A.I., Mikhailik, P.E., Mikhailik, E.V., Zarubina, N.V., Blokhin, M.G., 2015. Peculiarities of the distribution of rare-earth elements and yttrium in mineral phases of the ferromanganese crusts from the Detroit guyot (Pacific Ocean). *Dokl. Earth Sci.* 465 (2), 1243–1247.
- Koschinsky, A., Stascheit, A., Bau, M., Halbach, P., 1997. Effects phosphatization on the geochemical and mineralogical composition of marine ferromanganese crusts. *Geochim. Cosmochim. Acta* 61 (19), 4079–4094.
- Kronen, D., 1982. *Submarine Mineral Deposits* [in Russian]. Mir, Moscow.
- McLennan, S.M., 1989. Rare earth elements in sedimentary rocks: influence of provenance and sedimentary processes. *Rev. Mineral. Geochem.* 21 (1), 169–200.
- Melnikov, M.E., 2005. *Deposits of Cobalt-Bearing Manganese Crusts* [in Russian]. Yuzhmorgeologiya, Gelendzhik.
- Mikhailik, P.E., 2007. Ferromanganese crusts of submarine Belyaevsky and Medvedev volcanoes from the Sea of Japan, in: *Proc. 12th Int. Symp. WRI-12*. Balkema Publishers, Vol. 1, pp. 523–526.
- Mikhailik, P.E., Miroshnichenko, N.V., Lelikov, E.P., Barinov, N.N., 2004. Hydrothermal-sedimentary manganese deposits of submarine volcanoes from the Sea of Japan, in: *Minerals of the Ocean: Integrated Strategies-2*. St. Petersburg, pp. 173–175.
- Mikhailik, P.E., Derkachev, A.N., Chudaev, O.V., Zarubina, N.V., 2009. Fe–Mn crusts from underwater rises of the Kashevarov Trough (Sea of Okhotsk). *Russ. J. Pacific Geol.* 3 (1), 28–39.
- Mikhailik, P.E., Mikhailik, E.V., Zarubina, N.V., Barinov, N.N., S'edin, V.T., Lelikov, E.P., 2014a. Composition and distribution of REE in ferromanganese crusts of the Belyaevsky and Medvedev seamounts in the Sea of Japan. *Russ. J. Pacific Geol.* 8 (5), 315–319.
- Mikhailik, P.E., Khanchuk, A.I., Mikhailik, E.V., Zarubina, N.V., Blokhin, M.G., 2014b. New data on rare earth elements and yttrium distribution in hydrothermal Fe–Mn crusts from the Sea of Japan: Evidence from phase analysis. *Dokl. Earth Sci.* 454 (1), 79–83.
- Mikhailik, P.E., Mikhailik, E.V., Zarubina, N.V., Blokhin, M.G., 2014c. Peculiarities of Fe–Mn crusts composition from the Northwest Pacific seamounts, in: *Proc. 7th Conf. "Minerals of the Ocean"* Jointly with the 4th Conf. "Deep-Sea Minerals and Mining". St.-Petersburg, pp. 74–77.
- Mikhailik, P.E., Elovsky, E.V., Mikhailik, E.V., Blokhin, M.G., 2016. Rare earth elements and Y distribution in bottom sediments, in: *Deryugin Basin in the Barite Mountains Area in Oceanological Research*. *Proc. 7th Conf. Young Sci.* [in Russian]. *Dal'nauka, Vladivostok*.
- Mikhailik, P.E., Mikhailik, E.V., Zarubina, N.V., Blokhin, M.G., 2017. Distribution of rare-earth elements and yttrium in hydrothermal sedimentary ferromanganese crusts of the Sea of Japan (from phase analysis results). *Russian Geology and Geophysics (Geologiya i Geofizika)* 58 (12), 1530–1542 (1928–1943).
- Mills, R.A., Wells, D.V., Roberts, S., 2001. Genesis of ferromanganese crusts from the TAG hydrothermal field. *Chem. Geol.* 176 (1–4), 283–293.
- Murdmaa, I.O., Skornyakova, N.S. (Eds.), 1986. *Ferromanganese Concretions of the Central Pacific* [in Russian]. Nauka, Moscow.
- Prakash, L.S., Ray, D., Paropkari, A.L., Mudholkar, A.V., Satyanarayanan, M., Sreenivas, B., Chandrasekharan, D., Kota, D., Kamesh Raju, K.A., Kaisary, S., Balaran, V., Gurav, T., 2012. Distribution of REEs and yttrium among major geochemical phases of marine Fe–Mn-oxides: Comparative study between hydrogenous and hydrothermal deposits. *Chem. Geol.* 312–313, 127–137.

- Shterenberg, L.E., Aleksandrova, V.A., Gablina, I.F., 1986. Composition and structure of manganese crusts in the Sea of Japan. *Tikhookeanskaya Geologiya*, No. 1, 125.
- Skornyakova, N.S., Sval'nov, V.N., Murdmaa, I.O. (Eds.), 1989. *Ferromanganese Concretions of the Central Basin of the Indian Ocean* [in Russian]. Nauka, Moscow.
- Strakhov, N.M., Shterenberg, L.E., Kalinenko, V.V., Tikhomirova, E.S., 1968. *Geochemistry of the Sedimentary Manganese Ore Process* [in Russian]. Nauka, Moscow.
- Uspenskaya, T.Yu., Gorshkov, A.I., Gavrilenko, G.M., Sivtsov, A.V., 1989. Ferromanganese crusts and concretions of the Kuril Island Arc: structure, composition, and genesis. *Litologiya i Poleznye Iskopaemye*, No. 4, 30–40.
- Usui, A., Yuasa, M., Yokota, S., Nohara, M., Nishimura, A., Murakami, F., 1986. Submarine hydrothermal manganese deposits from the Ogasawara (Bonin) Arc, off the Japan Sea. *Mar. Geol.* 73 (3–4), 311–322.
- Usui, A., Bau, M., Yamazaki, T., 1997. Manganese microchimneys buried in the Central Pacific pelagic sediments: evidence of intraplate water circulation. *Mar. Geol.* 141 (1–4), 269–285.
- Zarubina, N.V., Blokhin, M.G., Mikhailik, P.E., Segrenev, A.S., 2014. Determination of the elemental composition of ferromanganese formations certified reference materials by mass-spectrometry with inductively coupled plasma. *Standartnye Obraztsy*, No. 3, 33–44.

Editorial responsibility: V.N. Sharapov